The Effect of Temperature on Fracture Energy of 3D Arc-Bend Specimen

Suvanit Chitsiriphanit[1,*]

[1] Department of Mechanical and Aerospace Engineering, Faculty of Engineering,
King Mongkut's University of Technology North Bangkok, Bangkok, Thailand 10800
*Corresponding Author: suvanitc@kmutnb.ac.th, Tel: 02 5870026, Fax: 02 5869541

Abstract

Temperature plays an important role on the fracture behavior of engineering materials. This paper presents the study of temperature effect on arc-bend specimen with various crack length ratio (a/W=0.2, 0.3, 0.4 and 0.5) under tensile loadings. The results at room temperature (25°c) and low temperature (-60°c) are obtained using numerical method. The simulation results of the normalized opening stress of 3D arc-bend specimens show that the slopes of the area close to the middle plane are nearly the same. When the ratio of distance measured from the middle plane to the specimen thickness (z/t) increases, the slopes keep decreasing and become more negative. The change of slopes can be observed evidently as the z/t ratio is larger than 0.4. Furthermore, it is found that the normalized fracture properties such as fracture toughness (K_I), strain energy release rate (G_I) and surface energy (γ_s) are close to unity for the z/t ratio between ±0.1 and these properties decrease continuously as it is approaching free surface in the thickness direction. At a temperature of -60°c, the increment of the a/W ratio causes the significant decrement in the fracture energy. The energy decreases remarkably when the z/t ratio reaches a value of ±0.4 approximately, in particular at temperature lower than room temperature. According to this study, it is obvious that the 3D specimen geometry at a different temperature will influence the stress state at the crack tip and the variations in the fracture properties.

***Keywords**:* Temperature, Stress state, Fracture surface energy and Fracture toughness

1. Introduction

The crack-like defect on the microscale generally means the presence of free surfaces. Based on the observation of these surface displacements, the elastic analysis shows that the stress distribution in the vicinity of crack tip will grow along the crack plane. Several researchers [1-3] have performed numerical technique to determine the difference between two and three-dimensional stress intensity factor of the cracked body. Tracey [1] found the variation of the degree of plane strain condition which affected the validity of stress intensity factor calculation. Rosakis and Ravi-Chandar [2] showed that the transition from two to three-dimensional analysis was half of the plate thickness away from the crack front. The relation between two-dimensional and three-dimensional analysis was proposed and also the meaning of the plane stress condition in relation to three-dimensional problem was examined by Kwon and Sun [3]. In addition, the influence of temperature on the local strain energy of blunted V and U notches in plane strain condition was examined by Gomez, et al. [4-6]. They conducted experiments under various types of specimens and found the good agreement between the experimental results and theory. In this paper, the effect of temperature and various sharp crack length ratio on fracture properties such as surface energy and fracture toughness of 3D arc-bend specimen under mode I loading was investigated in the thickness direction. Since no closed-form analytical approach was available for this study, finite element method was employed to analyze the variations in the fracture properties.

2. Dimensions of Arc-Bend Specimens

In order to explore the temperature effect on fracture energy, all the dimensions of arc-shaped tension model [A(T)] adapted from ASTM standard E399 were created. The specimens with four sizes of sharp crack length were considered along the symmetry plane.

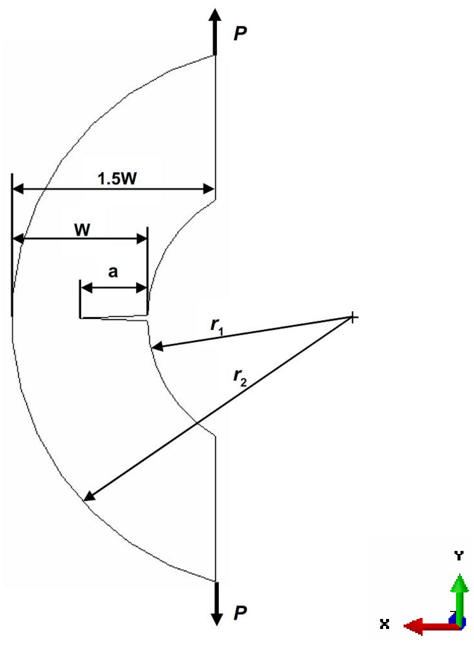

Fig. 1 Specimen Configuration of Arc-Bend [A(T)]

Fig. 1 displays the specimen configuration of the series of crack length ratio as listed in Table. 1. The thickness of the specimens was adequate so that antiplane was constrained (t=0.5W). The initial models with constant thickness (t=25 mm) ranged from a short crack length (a=10 mm) to a relatively long crack length (a=25 mm). The inner and outer radius of model were r_1=50 mm and r_2=100 mm respectively.

Table. 1 Dimensions of Arc-Bend Specimens

	a	W	a/W	r_1/r_2
Case 1	10	50	0.2	0.5
Case 2	15	50	0.3	0.5
Case 3	20	50	0.4	0.5
Case 4	25	50	0.5	0.5

In this research, polymethyl-methacrylate was used as the material in simulation. The material properties in case of plane strain condition are K_{IC}=1 $MPa\sqrt{m}$ at room temperature and K_{IC}=1.6 $MPa\sqrt{m}$ at the temperature of -60°c [4]. The details of research procedure will be described in the following section.

3. Computer Simulation

The results were obtained by numerical simulation in this work. The model was simulated under mode I fracture by applying a uniform displacement at the top part of the specimen.

3.1 Finite element model

Three-dimensional linear elastic models were created for all cases and discretized into small elements using FEM. Considering the symmetry of specimens, half of the symmetrical model was utilized for arc-bend containing crack with a small mesh size around the crack tip as shown in Fig. 2.

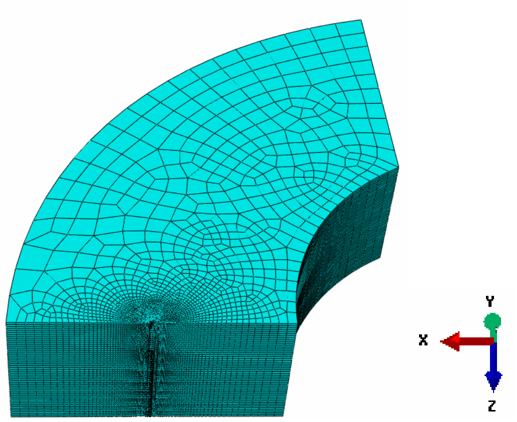

Fig. 2 Half Symmetry Model of Specimen and Mesh Used in FEM

A refined mesh density around the crack tip was kept uniform in order to compute strain energy release rate using three-dimensional modified crack closure method. In finite element model, the 8-noded hexahedral elements with the following mechanical properties: E = 3 GPa, ν = 0.3 at room temperature and E = 5.29 GPa, ν = 0.4 at the temperature of -60°c [4] were used in this analysis.

3.2 Stress distribution

To examine the stress state from finite element analysis, the total stress field (σ_{yy}) ahead of the crack tip can be obtained directly from simulation results.

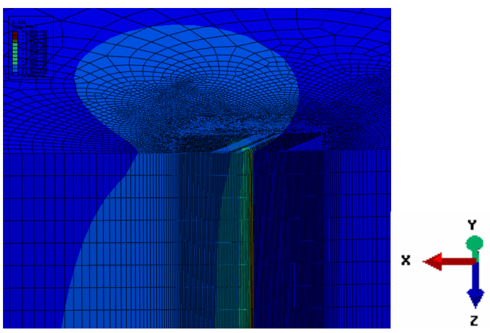

Fig. 3 Stress Distribution (σ_{yy}) along the Crack Plane for 3D Arc-Bend Specimen

The plot of three-dimensional opening stress state on the crack plane is presented in Fig. 3. Considering in the x-z plane, it appears from the figure that the opening stress distribution (σ_{yy}) is not constant across the symmetrical section. It tends to decrease from the middle plane continuously in the thickness direction. To give an explanation on this problem, Williams' asymptotic series expansion [7] was employed to represent the opening stress field ahead of the crack tip, which can be written as

$$\sigma_{yy} = \frac{K_I}{\sqrt{2\pi x}} + C_0\sqrt{x} + Higher\ order\ terms \quad (1)$$

The stress field in Eq. (1) consists of stress singularity combined with non-singular stress parts which are higher order terms. The value of the normalized opening stress varying along the thickness direction, where z position is measured from the middle plane, can be obtained by multiplying both sides with $\sqrt{2\pi x}/K_I$. Hence, the mathematical expression in Eq. (1) is rewritten as

$$\sigma_{yy}\sqrt{2\pi x}/K_I = 1 + \sqrt{2\pi}/K_I\,(C_0 x) + ... \quad (2)$$

The relationship of Eq. (2) is demonstrated by the following plots corresponding to different (z/t) positions.

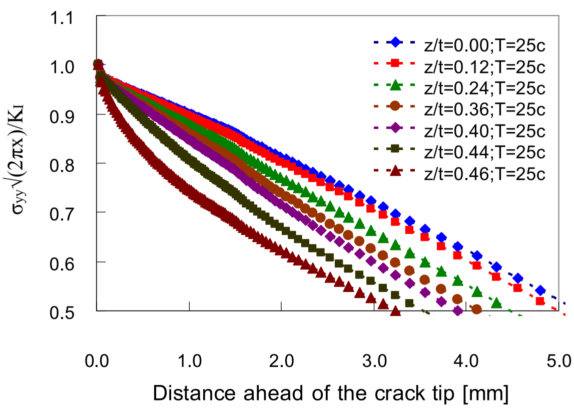

Fig. 4 Normalized Stress Distribution ahead of the Crack Tip (a/W=0.5 at T=25°c)

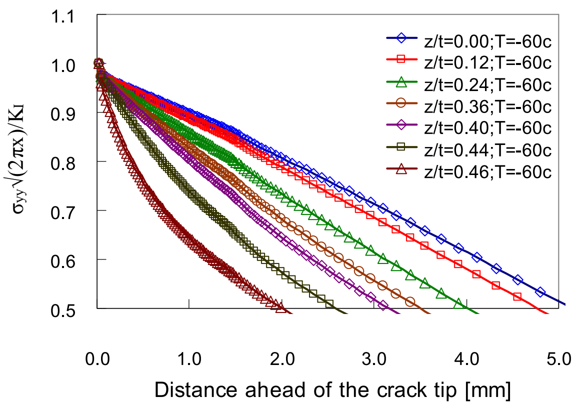

Fig. 5 Normalized Stress Distribution ahead of the Crack Tip (a/W=0.5 at T=-60°c)

It can be visualized from Figs. 4-5 that as the z/t ratio is approaching free surface (z/t=±0.5), the slopes are more negative. The simulation results of the normalized opening stress show that the slopes of the area close to the middle plane are nearly the same. With the same z/t ratio, the slope at the temperature of -60°c is less than the value at room temperature and the linear part represented by the second term on the right hand side of Eq. (2) is smaller as shown in the figure. The results exhibit that the slopes of the stress state decrease with the decreasing temperature.

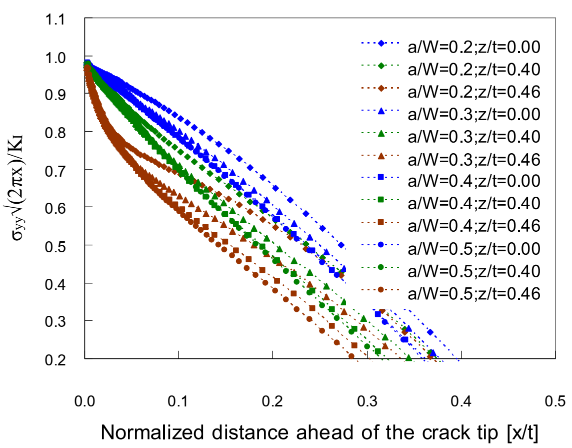

Fig. 6 Normalized Stress Distribution ahead of the Crack Tip (T=25°c)

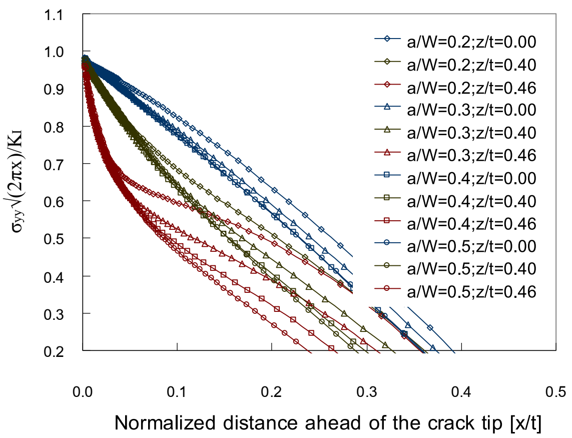

Fig. 7 Normalized Stress Distribution ahead of the Crack Tip (T=-60°c)

The slopes of all crack length ratio are plotted at the middle plane, the z/t ratio=0.40 and 0.46 as illustrated in Figs. 6-7. It clearly appears from the trends displayed at the same z/t ratio that the slopes are for the normalized opening stress with the tendency to decrease, in parallel with the decrement of temperature.

4. Numerical Calculation

In this section, fracture properties such as strain energy release rate, surface energy and fracture toughness will be computed using the resulting data obtained from the simulation.

4.1 Strain energy release rate

The most commonly used approach to study crack propagation is the Griffith's theory [8]. The strain energy release rate (G_I) is a parameter extensively used on fracture research to evaluate the Griffith condition when material will fail. The strain energy release rate can be computed using the modified crack closure method, first proposed by Rybicki and Kanninen [9] for two-dimensional problems. In order to capture the strain energy release rate along the thickness direction, the two-dimensional crack closure method can be modified to three-dimensional problems [10].

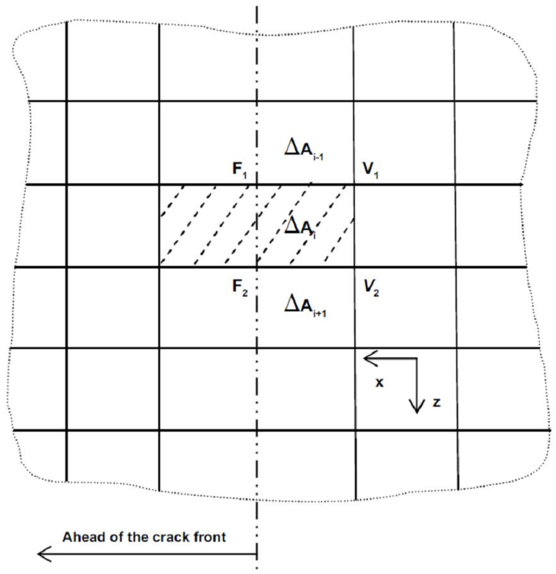

Fig. 8 Modified Crack Closure Method for 3D

A schematic representation of a finite element for a cracked model using 8-noded linear hexahedral elements along the crack front is depicted in Fig. 8. The areas of elements (i+1), (i) and (i-1) in the x-z plane are ΔA_{i+1}, ΔA_i and ΔA_{i-1} respectively. The strain energy release rate of i^{th} element can be obtained from the following relationship

$$G_i = \frac{1}{2\Delta A_i}\left(F_1^i v_1 + F_2^i v_2\right) \tag{3}$$

In this equation, v_1 and v_2 are the opening displacements behind the crack front. The F_1^i and F_2^i are the nodal forces at the crack front corresponding to the i^{th} element.

$$F_1^i = \frac{\Delta A_i}{\Delta A_{i-1} + \Delta A_i} F_1 \tag{4}$$

$$F_2^i = \frac{\Delta A_i}{\Delta A_i + \Delta A_{i+1}} F_2 \tag{5}$$

The F_1^i and F_2^i can be calculated from F_1 and F_2 in conjunction with the adjacent areas as given in Eqs. (4)-(5).

4.2 Surface energy

As mentioned earlier, an increase in surface energy (γ_s) causes the strain energy for crack growth. The critical strain energy (G_c) required to create two new surfaces is equivalent to elastic energy release rate by crack extension, which is expressed as

$$G_c = 2\gamma_s \tag{6}$$

in which γ_s is the surface energy of cracked body for arc-bend model with two surfaces and one crack tip.

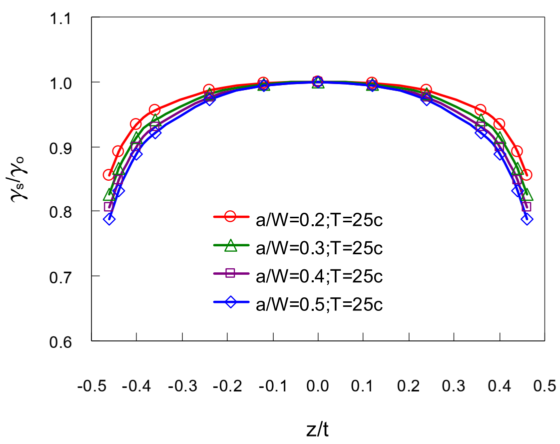

Fig. 9 Normalized Surface Energy (T=25°c) in the y-z Plane

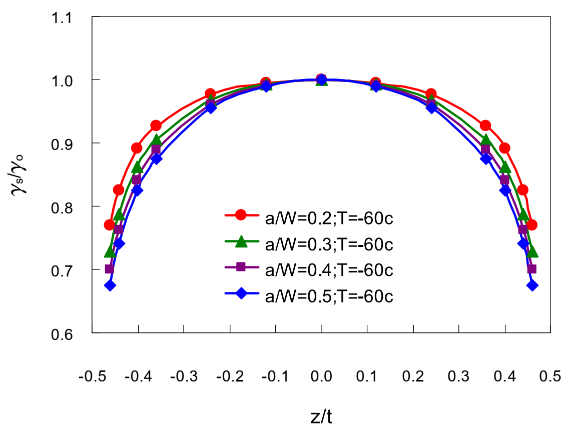

Fig. 10 Normalized Surface Energy (T=-60°c) in the y-z Plane

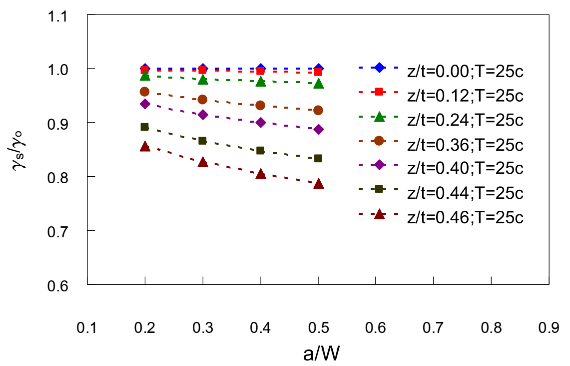

Fig. 11 Normalized Surface Energy (T=25°c) in the x-y Plane

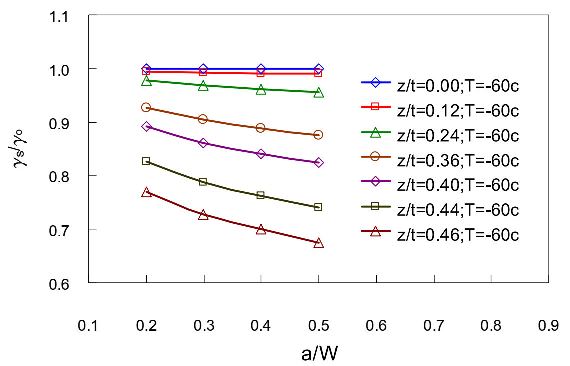

Fig. 12 Normalized Surface Energy (T=-60°c) in the x-y Plane

Figs. 9-10 present the surface energy normalized with respect to the value at the middle plane (γ_s/γ_0) for each case in the y-z plane. It can be noted that normalized surface energy keeps decreasing as the z/t ratio is away from the middle plane. When this ratio is larger than 0.4 approximately, the great reduction of normalized surface energy can be seen apparently at the temperature of -60°c. Considering the plots in the x-y plane as shown in Figs. 11-12, the increase of crack length ratio (a/W) results in the significant decrement of normalized surface energy near free surface. This phenomenon is more evident in higher crack length ratio.

4.3 Fracture toughness

In previous section, strain energy release rate was obtained by three-dimensional modified crack closure method. This value can be converted to fracture toughness using the correlation between G and K for plane strain condition given as

$$G_I = \frac{K_I^2(1-\nu^2)}{E} \qquad (7)$$

where E is Young's modulus and ν is Poisson's ratio of material. The following plots illustrate the fracture toughness normalized with respect to the value at the middle plane (K_I/K_0) and represented in the three-dimensional view.

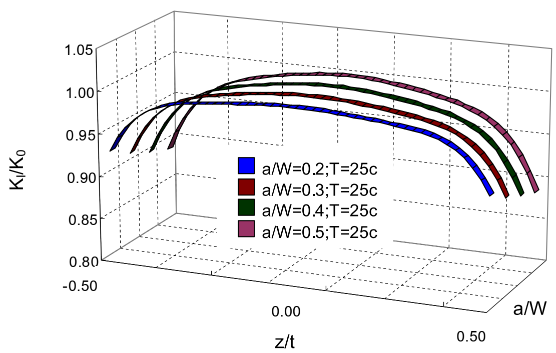

Fig. 13 Normalized Fracture Toughness (T=25°c) in the Three-Dimensional View

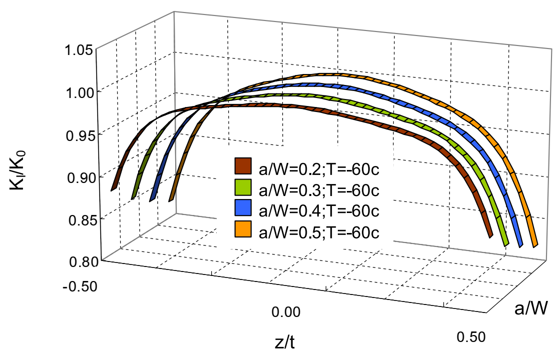

Fig. 14 Normalized Fracture Toughness (T=-60°c) in the Three-Dimensional View

By comparing Figs. 13-14, the three-dimensional graphs demonstrate the temperature dependence of normalized fracture energy of specimens with the series of crack length ratio. Considering the same z/t ratio along the thickness direction, it is apparent to note that the normalized fracture toughness continues to decrease corresponding to the increase of crack length ratio from a/W=0.2 to 0.5. Additionally, it can be observed that the variations in the temperature dependent fracture energy are caused by the different temperature. That is, at the temperature of -60°c, the normalized fracture toughness near free surface is less than the value at room temperature. From the plots as presented in Figs. 9-14, the findings are clearly revealed that the temperature and specimen geometry with various crack length play the foremost role in fracture energy.

5. Conclusions

In the present study, numerical analysis of polymethyl-methacrylate was performed at a different temperature. The fracture energy of three-dimensional arc-shaped bend specimen was examined. Considering along the thickness direction, it was shown that as the z/t ratio was between ± 0.1, the slopes of the normalized opening stress were nearly the same and the normalized surface energy remained close to unity. When the z/t ratio was larger than 0.4 approximately, the significant decrement of slopes and normalized fracture energy was more evident near free surface. Comparison of the different temperature, it was also found that the temperature lower than room temperature resulted in the decreasing of the normalized fracture toughness consistent with the opening stress state. Moreover, the resulting simulation at the temperature of -60°c showed the reduction of the normalized fracture toughness obviously with increasing the crack length ratio. As a result, the variations in fracture properties were mainly dependent on the temperature and specimen geometry.

6. References

[1] Tracey, D.M. (1974). Finite elements for three-dimensional elastic crack analysis, *Nuclear Engineering and Design*, vol. 26, 1974, pp. 282-290.

[2] Rosakis, A. and Ravi-Chandar, K. (1986). On crack-tip stress state: an experimental evaluation of three-dimensional effects, *International Journal of Solids and Structures*, vol. 22, 1986, pp. 121-134.

[3] Kwon, S.W. and Sun, C.T. (2000). Characteristics of three-dimensional stress fields in plates with a through-the-thickness crack, *International Journal of Fracture,* vol. 104, 2000, pp. 291-315.

[4] Gomez, F.J. and Elices, M. (2004). A fracture criterion for blunted V-notched samples, *International Journal of Fracture*, vol. 127, 2004, pp. 239-264.

[5] Lazzarin, P. and Berto, F. (2005). Some expressions for the strain energy in a finite volume surrounding the root of blunt V-notches, *International Journal of Fracture,* vol. 135, 2005, pp. 161-185.

[6] Gomez, F.J., Elices, M., Berto, F. and Lazzarin, P. (2007). Local strain energy to assess the static failure of U-notches in plates under mixed mode loading, *International Journal of Fracture,* vol. 145, 2007, pp. 29-45.

[7] Williams, M.L. (1957). On the stress distribution at the base of a stationary crack,

Journal of Applied Mechanics, vol. 24, 1957, pp. 109-114.

[8] Griffith, A.A. (1920). The phenomena of rupture and flow in solids, *Philosophical Transactions of the Royal Society of London*, vol. A-221, 1920, pp. 163-197.

[9] Rybicki, E.F. and Kanninen, M.F. (1977). A finite element calculation of stress intensity factors by a modified crack closure integral, *Engineering Fracture Mechanics*, vol. 9, 1977, pp. 931-938.

[10] Shivakumar, K.N., Tan, P.W. and Newman Jr., J.C. (1988). A virtual crack-closure technique for calculating stress intensity factors for cracked three dimensional bodies, *International Journal of Fracture*, vol. 36, 1988, pp. R43-R50.